Model physics influences on tropical cyclone size

YIZHE PEGGY BU AND ROBERT G. FOVELL

Department of Atmospheric and Oceanic Sciences, University of California, Los Angeles

ABSTRACT

Using a semi-idealized version of the operational Hurricane WRF (HWRF) model, we show that model physical parameterizations can dramatically influence TC size (width) as measured by the 34-kt near-surface wind radius. Enabling cloud-radiative forcing and enhancing planetary boundary layer vertical mixing can both lead to wider storms via encouraging more convective activity in the TC's outer region, the heating from which broadens the wind field. These two processes can cooperate or compete, and are dependent on favorable environmental conditions, complicating the evaluation of model physics improvements. An alternative approach to limiting hurricane inner core mixing in the GFS scheme without unrealistically discounting mixing outside the TC is presented.

1. Introduction

TC size is an important forecast metric for it directly and indirectly influences TC motion, intensity, track, and storm surge. In meteorology, there are a variety of metrics used to define the TC size such as the radius of outermost closed isobar, the radius of vanishing wind and the radius of 34-knot (kt) wind speed. In this study, the radius of 34-kt (about 17 m s^{-1}) wind speed at 10 m above mean sea level (MSL) is used to define the storm size or width.

Bu et al. (2014) and Fovell and co authors (2015) demonstrated that the cloud-radiative forcing (CRF), the interaction of hydrometeors with longwave and shortwave radiation, has an important role in expanding the storm radius. Averaged through a diurnal cycle, CRF consists of pronounced cooling along the anvil top and weak warming through the cloudy air. In particular, the within-cloud warming was relevant, enhancing convective activity in the TC outer core, leading to a wide eye, a broader tangential wind field, and a stronger secondary circulation. This forcing also functions as a positive feedback, assisting in the development of a thicker and more radially extensive anvil than would otherwise have formed. CRF itself depends on the microphysics parameterization and Fovell et al. (2010) showed it is a major reason why simulations can be sensitive to microphysical assumptions.

Bu et al. (2014) also showed that the GFDL-derived radiation scheme employed operationally in the Hurricane Weather Research and Forecasting (HWRF) model (Gopalakrishnan et al. 2012) since its inception did not handle CRF properly, resulting in deep clouds that were effectively transparent. However, testing revealed that implementing an ostensibly superior radiation scheme *degraded* model skill. Analysis of those results led us to consider how planetary boundary layer (PBL) mixing influences storm size, in cooperation and competition with CRF.

It is widely appreciated that PBL processes play an important role in tropical cyclones (e.g., Smith 1968; Ooyama 1969; Emanuel 1986; Van Sang et al. 2008) and there have been many studies addressing the sensitivity of simulated TC to PBL schemes (e.g., Braun and Tao 2000; Hill and Lackmann 2009; Nolan et al. 2009a,b; Smith and Thomsen 2010). Most previous studies focusing on the PBL-TC relationship have focused on TC intensity, inner core convection and/or the TC PBL structure. Our interest is in the influence of PBL mixing on horizontal storm structure and size, and we utilize the GFS PBL scheme because this is employed in the operational HWRF. This is a first-order vertical diffusion scheme based on Troen and Mahrt (1986) and Hong and Pan (1996), which also gave rise to the commonly used YSU PBL scheme.

In the GFS scheme, the PBL depth h is determined using an iterative bulk-Richardson approach calculated from the ground upward. The vertical profile of momentum eddy diffusivity K_m is then obtained via

$$K_m = k(U_*/\phi_m)Z[\alpha(1 - Z/h)^2], \qquad (1)$$

where k is the von Kármán constant (= 0.4), U_* is the surface frictional velocity scale, ϕ_m is the wind profile function evaluated at the top of the surface layer, and Z is the height above the surface. This produces a mixing coefficient profile that is parabolic in shape between the surface and height h.

A recent addition is the tuning parameter, α, which was incorporated because Gopalakrishnan et al. (2013) determined the GFS scheme was producing a negative bias in storm intensity and positive bias in inner core boundary layer depth in HWRF, a consequence of excessively large K_m values relative to those estimated from observations by Zhang et al. (2011b). Figure 1, taken from Gopalakrishnan et al. (2013), demonstrates how the α parameter can control the simulated K_m as a function of wind speed. While a value of $\alpha = 0.25$ (Fig. 1b) was found to produce the most reasonable results relative to the observations for wind speeds in the range 10 - 60 m s^{-1}, a value of $\alpha = 0.7$ was adopted in the 2013 and 2014 operational versions of HWRF in all three of its telescoping domains as a consequence of detailed skill testing against retrospective TC cases.

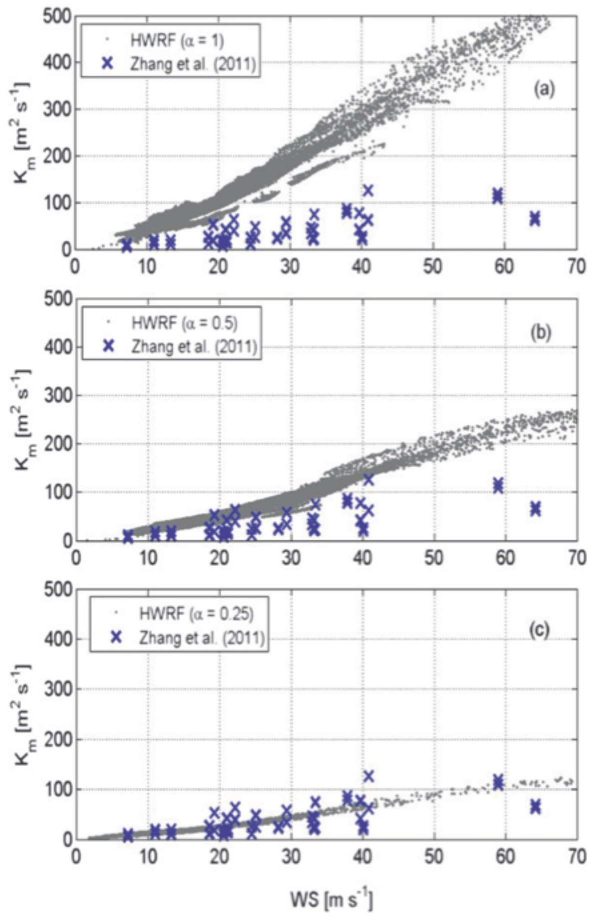

Fig. 1. The variation of the eddy diffusivity coefficient at about 500 m MSL with 10-m wind speed from high-resolution HWRF model output (grey dots) using α values of (a) 1, (b) 0.5, and (c) 0.25, compared with observationally-derived values from Zhang et al. (2011a) (purple crosses). From Gopalakrishnan et al. (2013).

2. Model and experimental design

The simulations of this study are carried out using the 2013 version of the HWRF model, similar to that used in Bu et al. (2014). These experiments are "semi-idealized" in that we dramatically simplified the operational configuration to exclude land and decouple the ocean model, employ a uniform and constant sea-surface temperature (SST), and initialize with a horizontally homogeneous tropical sounding without any mean flow. The “bubble” procedure described in Cao et al. (2011) was used to initiate the TC. All HWRF simulations spanned four days and composite model fields were constructed for the fourth day in a vortex-following fashion, averaging over one full diurnal cycle, and all fields shown herein are azimuthally averaged.

As in Bu et al. (2014), we adopted the 2012 HWRF design of three telescoping domains (with 27, 9 and 3 km horizontal grid spacings) along with some of the operational model physics used during the 2013 season, such as the SAS (Simplified Arakawa-Schubert) cumulus parameterization (in the 27 and 9 km domains after 24 h) and the aforementioned GFS PBL scheme. The “operational configuration” also consisted of a tropical variant of the Ferrier et al. (2002) microphysical parameterization (MP) and the GFDL radiation package; this is compared to runs made using the Thompson et al. (2008) MP and/or RRTMG radiation (Iacono et al. 2008).

3. Results

a. *Cooperation with CRF*

As mentioned above, Bu et al. (2014) demonstrated that CRF plays an important role in determining TC structure. Enabling CRF can increase the storm size (as manifested by the 34-kt radius of the 10-m wind speed) by a substantial (and MP-dependent) amount (compare thin blue and thin red contours in Fig. 2) because hydrometers interacted with radiation to force gentle ascent, elevating the relative humidity through a deep layer mainly above the PBL. When the RRTMG scheme was employed, both the operational (Ferrier) and a more sophisticated (Thompson) microphysics schemes permitted generation of realistic patterns of SW warming and LW cloud-top cooling and within-

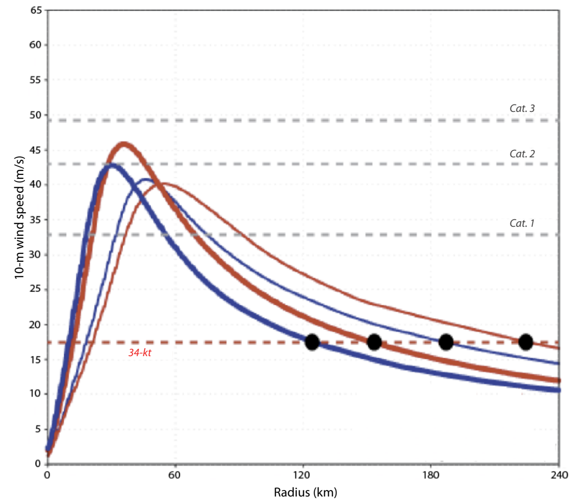

Fig. 2. Radial profiles of the azimuthally-averaged 10-m wind speed from semi-idealized HWRF simulations using Ferrier MP with GFDL radiation and α=0.7 (operational configuration; thin blue contour); RRTMG radiation and α=0.7 (thin red contour); RRTMG and α=0.25 (thick red contour); and GFDL and α=0.25 (thick blue contour). Black dots indicate 34-kt wind radii.

cloud warming, with variations in pattern and magnitude reflecting the different assumptions employed by the MPs (shown for Thompson in Fig. 3a). Note there is no effective CRF with the operational GFDL radiation package (Fig. 3b).

After we identified the CRF issue, the Developmental Testbed Center (DTC) and the HWRF team evaluated the RRTMG scheme along with Thompson microphysics for adoption in the operational HWRF. Analyses of retrospective simulations demonstrated that the HWRF forecast skill was generally degraded when the new physics was included and, as a consequence, neither package was adopted for the 2014 TC season. Our analyses of their experiments led us to realize that both CRF and PBL mixing have potentially profound influences on storm structure, which can directly and indirectly influence intensity and track forecast skill. In brief, CRF encourages convective activity in the outer core via gentle lifting above the PBL, but outer region convection can also result from enhanced vertical mixing within the PBL – controlled by the α parameter – which carries moisture from the sea surface to the top of the boundary layer. In both cases, the enhanced convective activity in the outer region broadens the wind field, as shown by Bu et al. (2014) and Fovell and co authors (2015).

It emerges that these two processes, CRF and PBL mixing, can cooperate or compete. Recall that Gopalakrishnan et al. (2013) recommended a value of $\alpha = 0.25$ in (1), but 0.7 was selected for operational use. Our working hypothesis was that this increased α inadvertently compensated for the model's tendency to produce overly small TCs, *which was actually a consequence of the missing CRF*. Therefore, when the radiation problem was fixed, the model was left with a fairly consistent positive size bias that led to worse skill scores[1]. Put another way, we believe that a proper implementation of CRF would justify a smaller and more defensible (based on the observations) value of vertical eddy mixing in the GFS PBL.

We now demonstrate that CRF and α have qualitatively similar influences on horizontal storm size. Figure 2 also shows the effect of different combinations of CRF and PBL mixing on TC width for Ferrier-based storms. Note varying α (for fixed CRF) causes the 34-kt wind radius to increase by about 75% independent of the radiation scheme employed (compare thick and thin contour pairs). The narrowest storm used the $\alpha = 0.25$ value suggested by Gopalakrishnan et al. (2013) with GFDL radiation, while the widest employed the operational setting (0.7) with RRTMG. Thus, it is seen that the physics interplay between CRF and mixing can alter the 34 kt wind radius by factor of two, which is dramatic. There is a material impact on the eye size as well.

[1]Among the 2012 retrospective hurricanes examined, the positive size bias was readily apparent among the Atlantic storms. In the East Pacific, the Thompson/RRTMG cases tended to exhibit positive biases early on, but also encountered colder SSTs earlier, resulting negative size biases at longer forecast lead times.

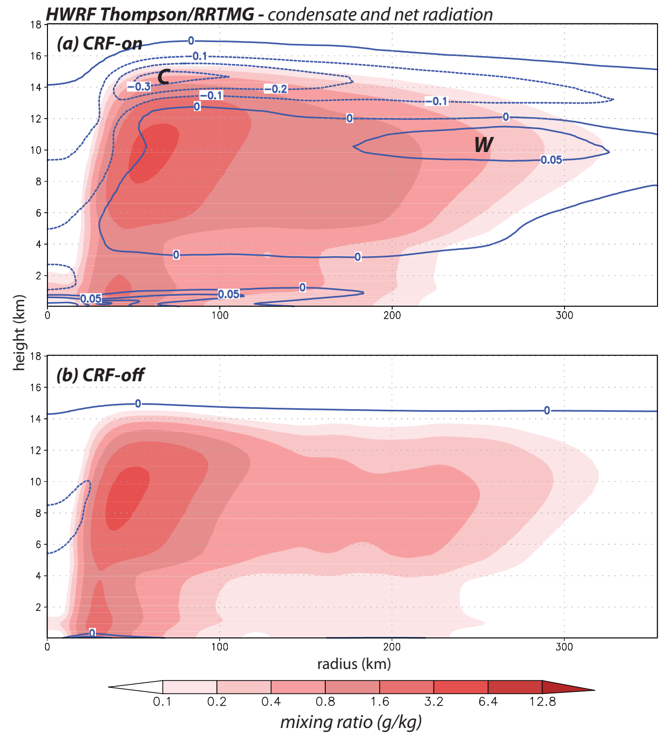

FIG. 3. Total condensation (shaded, note logarithmic scale) and net radiation (negative [dashed] contour interval 0.1 K h^{-1}, and positive [solid] interval 0.05 K h^{-1}) for Thompson storms with (a) RRTMG, and (b) GFDL radiation. C and W stand for cooling and warming, respectively. From Bu et al. (2014).

b. Eddy diffusion and storm size

1) SENSITIVITY TO α

The foregoing result occurs because the PBL mixing acts in a very similar manner as CRF in expanding storm size, as illustrated in Fig. 4, which also focuses on the Ferrier MP. The shaded field is net diabatic forcing owing to microphysics, temporally and azimuthally averaged. Implementing CRF for fixed α (left column) and varying α for fixed CRF (right column) both result in a radially expanded heating field, causing the wind field (as illustrated by tangential wind differences in the bottom row) to expand. Note that for this MP, sensitivity to α exceeds that for CRF, as was suggested by the near-surface wind profiles (Fig. 2).

The α parameter was added to (1) to control

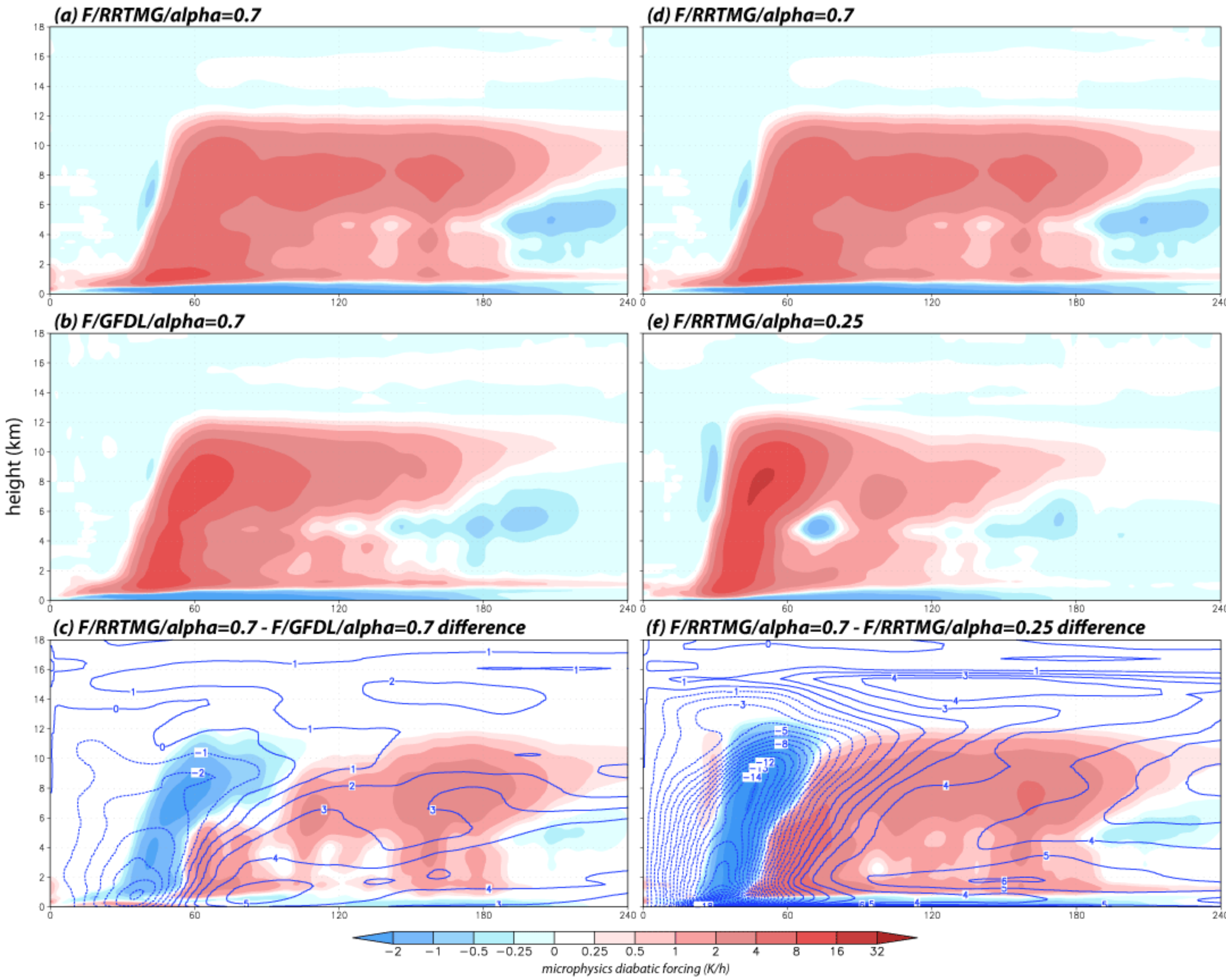

FIG. 4. Radius vs. height cross-sections showing the symmetric components of microphysics diabatic forcing (shaded at K hr^{-1}) and tangential wind (contoured at 10 m s^{-1}) from Ferrier MP simulations and α=0.7 for the (a) RRTMG radiation and (b) GFDL radiation cases. Panel (c) shows the RRTMG minus GFDL difference fields; the superposed field is tangential velocity difference (1 m s^{-1} contours). Also shown are simulations using Ferrier MP and RRTMG radiation with (d) α=0.7 and (e) α=0.25. Panel (f) shows the α=0.7 minus α=0.25 difference fields.

eddy mixing in the hurricane inner core. Owing to its implementation, mixing is reduced throughout the hurricane and beyond. Figure 5 shows vertical profiles of K_m, averaged over an annulus residing between 30 and 200 km from the center for various α values, with the corresponding near-surface wind profiles presented in Fig. 6. The simulations in these figures employed Thompson MP, RRTMG radiation, and CRF was active, along with our default sea surface temperature (SST) of 302.5 K. Note that the K_m profiles differ little with respect to vertical shape, which is determined by (1) and the PBL depth h. Varying α from 0.25 to 1.0, however, causes the storm size to increase monotonically from 150 km to 250 km.

One important and direct impact of the eddy mixing is associated with the vertical transport of water vapor in the boundary layer, upward from the sea surface to the PBL top. Figure 7 presents averaged vapor and K_m fields for Thompson/RRTMG storms with α=0.7 and 0.25, along with their differences. Note the latter demonstrate that the more substantial mixing produced with larger α is associated with higher moisture contents in the upper portion of the PBL, especially at larger radii. This pattern is consistent with the contribution of vertical eddy mixing to the local vapor tendency, which is a second-order parabolic term (Klemp and Wilhelmson (1978)) of the form

$$\left[\frac{\partial q}{\partial t}\right]_{mix} = \frac{\partial}{\partial z} K_h \frac{\partial q}{\partial z} \qquad (2)$$

where q is the water vapor mixing ratio, z is the height, and K_h is the vertical diffusion applied to scalars such as moisture and potential temperature (and nearly identical to K_m for these situations).

In the atmosphere, the water vapor concentration decreases quasi-linearly with height and, as a consequence of the parabolic vertical shape of K_h, we would expect negative vapor tendencies where K_h increases with height (below the level where K_h reaches its maximum) and positive tendencies where K_h decreases with height (above the K_h maximum). This also applies to the difference fields, and explains the positive values above, and negative ones below, the level of maximum K_m difference (Fig. 7c). Thus, one contributor leading to the greater PBL moisture ($\geq$ 400 m above the sea surface) in the larger α run is enhanced vertical mixing. The enhanced water vapor transport to the top of the PBL brings the air there closer to saturation, which can encourage more convective activity, producing the diabatic heating that eventually leads to a broader wind field.

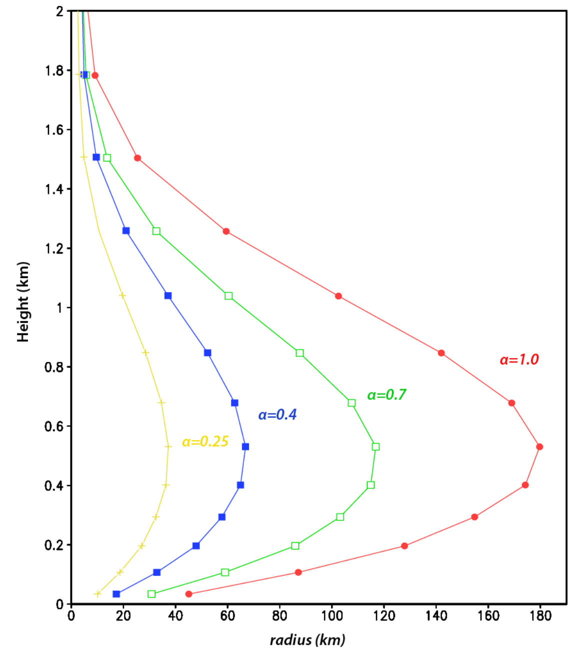

FIG. 5. Vertical profiles of eddy diffusivity (K_m, m^2 s^{-1}) averaged from radius of 30 to 200 km of simulations using GFS PBL scheme with α=1.0 (red), α=0.7 (green), α=0.4 (blue), and α=0.25 (yellow).

2) Sensitivity to SST

Examination of DTC's HWRF retrospective cases from their initial Thompson/RRTMG tests described above suggested to us that the impact of α could vary from case to case, and even from region to region, with some storms being quite insensitive to the value employed. From these cases, we surmised that the less convectively favorable the environment, the less influence eddy

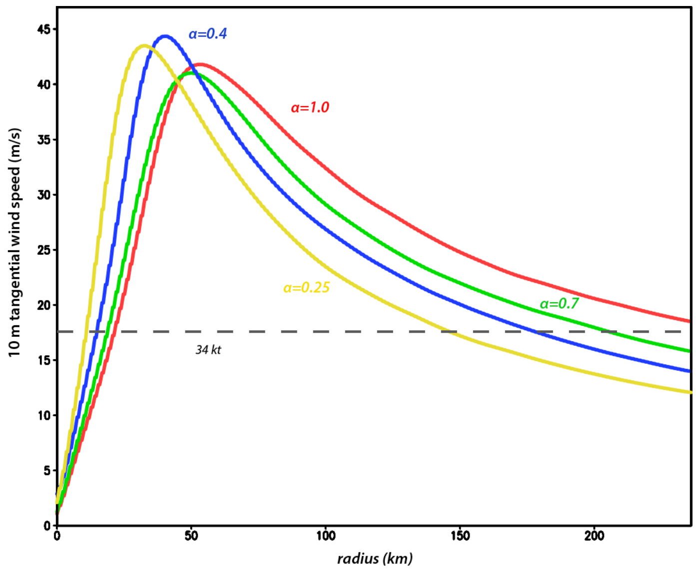

FIG. 6. 10-m wind speed(m s^{-1}) as a function of the radius of simulation with α=1.0 (red), α=0.7 (green), α=0.4 (blue), and α=0.25 (yellow).

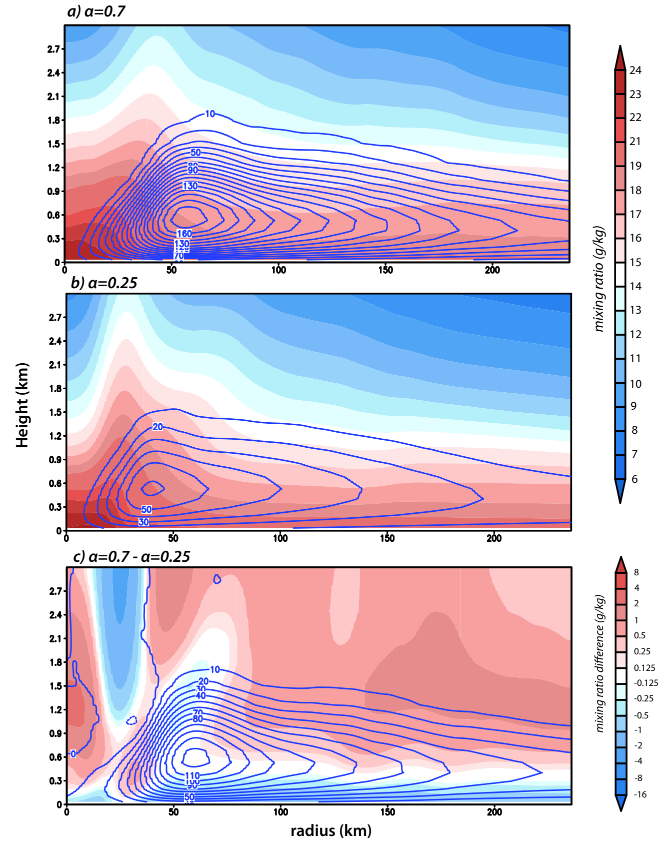

FIG. 7. Radius vs. height cross-sections showing the symmetric components of water vapor (shaded, g kg^{-1}) and eddy diffusivity applied to vapor K_h (10 m^2 s^{-1} contours), for Thompson/RRTMG simulations using (a) α=0.7; (b) α=0.25; and (c) the differences between the two. Simulations used SST=302.5 K.

mixing of moisture would or could have. Within the semi-idealized framework, we can establish a less favorable environment for convection by simply lowering the SST. In this section, we explore how SST controls the impact of α on the storm size.

For example, when the sea surface is cooled by 2.5 K (Fig. 8b), to 300 K, the size difference between the α=0.7 (black curve) and the α=0.25 (red curve) storms is smaller than when the SST was set to 302.5 K (Fig. 8a). (Curiously, the *intensity* difference is larger at this more moderate surface temperature; we speculate about this below.) When the SST is further reduced to 298 K, the TC size difference almost vanishes (Fig. 8c). Figure 9 presents the vapor and K_m difference fields between large and small α runs for these two cooler SSTs, for comparison with Fig. 7c. The overall patterns are similar but the magnitudes are smaller. Reduced eddy mixing, especially in the outer core region, leads to reduced vertical vapor transport, resulting in less convective activity. As a result, other factors being equal, the wind field could not be expanded as much.

Thus, it appears that TC size can be directly modulated via water vapor transport in the boundary layer, with the size differences between the TCs produced by larger and smaller α values gradually disappearing as the entropy supply from the sea surface is reduced. The inclusion of lower sensitivity cases could serve to obscure the influence of α somewhat in ensemble statistics spanning a large number of events. In contrast, the intensity differences emerge as somewhat more complex. Greater vertical transport in the outer core region will always encourage larger TCs, but TC intensity can be influenced by the competition between the strength of the convection in the eyewall and outer core regions. Though decreasing the water vapor diffusion through the whole

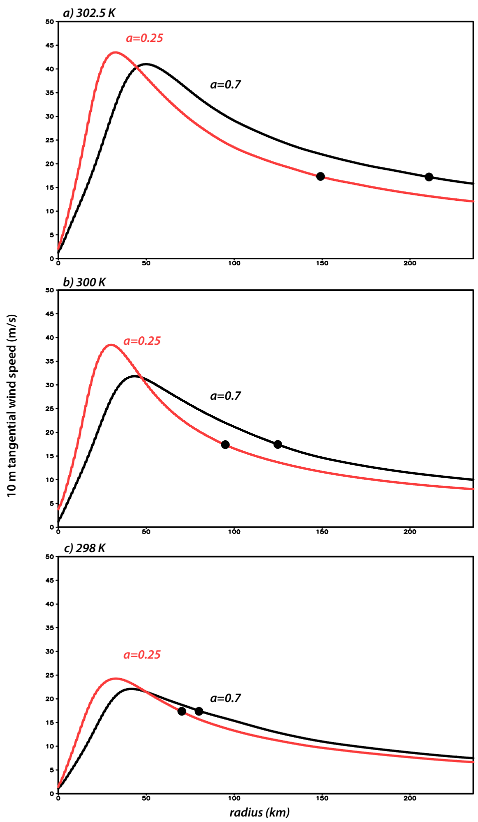

FIG. 8. 10-m wind speed (m s^{-1}) as a function of radius for Thompson/RRTMG simulations with α=0.7 (black) and α=0.25 (red) and (a) SST=302.5 K; (b) SST=300 K; and (c) SST=298K.

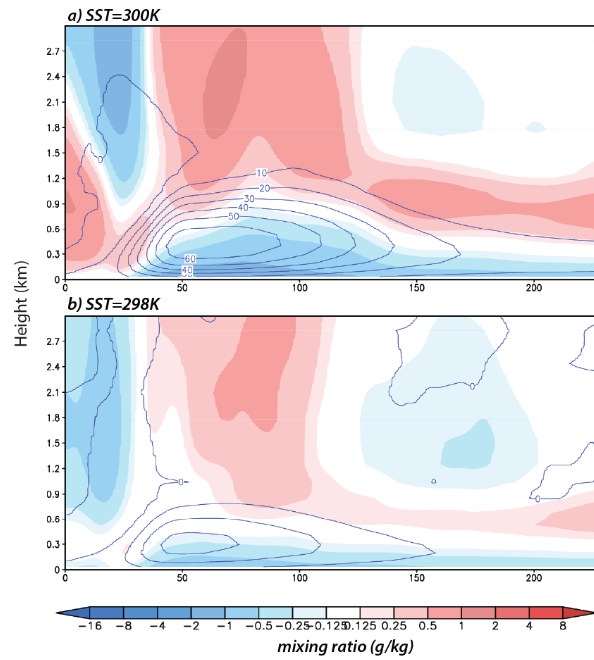

FIG. 9. As in Fig. 7c, but showing vapor and K_h difference fields between α=0.7 and α=0.25 simulations with (a) SST=300 K; and (b) SST=298 K.

domain may suppress the convection in the eyewall region somewhat, the outer convection may be reduced even more. As a consequence, the net influence may be to actually intensify the TC. This would require further study.

c. *An empirical cap for eddy diffusivity*

1) Motivation

As mentioned above, the operational HWRF's GFS PBL scheme can produce values of eddy momentum diffusion (K_m) that are much greater than suggested by observations (Zhang et al. 2011a,b; Gopalakrishnan et al. 2013), especially when the wind speeds are large. To ameliorate this, the α factor was introduced into the eddy diffusivity equation (1) to tune the PBL-generated mixing, although a larger value for this parameter than suggested by the observational comparison was eventually adopted for the operational model. We have shown that α not only can strongly modify TC inner core structure, but also may influence the outer wind field. However, the adoption of this mixing reduction factor comes with some problems.

First of all, the imposition of a constant α value does not guarantee that K_m will not exceed the observed values in some cases and at some wind speeds. Additionally, it introduces another model "knob" that requires tuning, and the α value which is optimal for the inner core region may not be best for the outer core region. When $\alpha = 0.7$, the simulated storm might be too weak with an excessively deep PBL. A value of $\alpha = 0.25$ might lead to the storm with the correct intensity but is too narrow. It is likely impossible to get a universal α value which can "fit" for every case.

Most worrisome of all, this original implementation of α means that eddy mixing is reduced relative to the default GFS scheme not only within the hurricane inner core but also through the entire domain. That is, α affects mixing over the ocean far from the TC, and over land, places where the PBL scheme should not be modulated (if the scheme is fundamentally accurate). To address these issues, we have designed a new computational algorithm to limit the vertical mixing in the TC's inner region as indicated by the observations but without artificially constraining the scheme in the surrounding environment or changing the vertical shape of the eddy diffusivity profile generated by the PBL scheme. The new scheme is applied only over water, and even then is likely to activate only when wind speeds of the kind found in hurricane inner cores are encountered, leaving the PBL scheme unmodified for the vast majority of grid points.

2) Approach and implementation

This is achieved through imposition of a wind speed-dependent upper bound on K_m based on the diagnosed eddy diffusivity at 500 m MSL derived from the Zhang et al. (2011b) observations (Fig. 1). According to the correlation between the wind speed (WS) and the K_m value at 500 m as revealed in Fig. 10, we consider WS/0.6 as a simple, observationally-suggested, and empirical "cap" for K_m to enforce an upper bound on eddy mixing based on wind speed, which will act to limit K_m in the inner core where wind speeds are large. In this strategy, α in (1) is transformed into a wind speed-dependent reduction factor that will vary from column to column, being effectively inactive (i.e., $\alpha = 1$) in many of them. The strategy is carried out via the following steps, with some possible scenarios depicted in Fig. 11.

First, we determine the wind speed at the model level nearest 500 m above the surface in each model column and then calculate K_m(cap) as WS/0.6 for that column. Next, the first guess K_m is computed by the PBL scheme using (1) without modification ($\alpha = 1$). If K_m at 500 m $\leq$ K_m(cap) for any reason, then K_m remains at its first guess value and mixing is unrestricted. [As illustrated in Fig. 11a and b, it does not matter that K_m might exceed the capping value above or below 500 m, as the observations only constrain the mixing at the 500 m level]. If, however, K_m at 500 m exceeds the cap, then the α for that column is K_m(cap)/K_m(500 m). This α is then applied through the entire PBL within that model column to shift the eddy diffusivity profile leftward (to smaller mixing coefficient values) without change of shape (as illustrated by the dashed curves in Fig. 11c and d). Note that this strategy permits this "effective α" to vary in space.

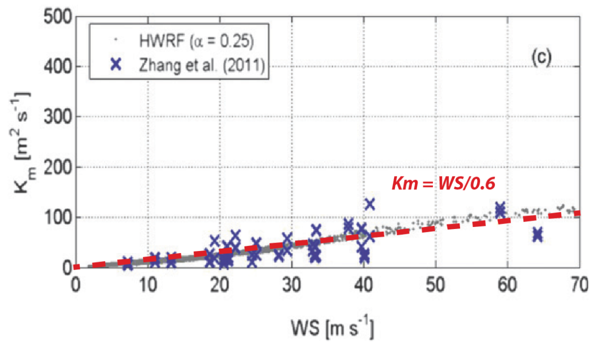

Fig. 10. Same as Fig.1c, but the red dashed line of K_m=WS/0.6 superimposed by the authors as the proposed wind speed-based limit on K_m.

3) Results

Figure 12a presents a scatterplot of wind speed against the eddy mixing at 500 m MSL for semi-idealized Ferrier/RRTMG simulations, averaged not only temporally and azimuthally but also through a 150 km wide annulus extending outward from the radius of maximum wind (RMW). By design, the capped K_m profile (purple) does not exceed the WS/0.6 limit (dashed) although there is nothing to prevent K_m from being less than the cap. In this particular situation, the α=0.4 case roughly follows along the WS/0.6 limit, but this is strongly case-dependent (see below) and thus not guaranteed. As α gets larger, K_m increases at a faster rate as wind speed strengthens, and α values such as 0.7 and larger result in very large

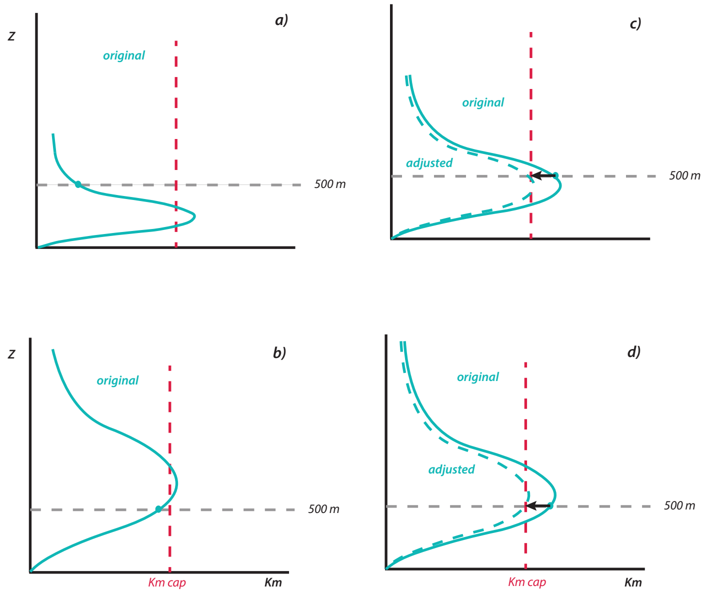

FIG. 11. Depiction of K_m adjustment based on K_m(500 m) and K_m(cap) for scenarios in which: (a) the height of maximum K_m is below 500 m but $K_m(500 \text{ m}) < K_m(\text{cap})$; (b) the height of maximum K_m is above 500 m but $K_m(500 \text{ m}) < K_m(\text{cap})$; (c) the height of maximum K_m is below 500 m and $K_m(500 \text{ m}) > K_m(\text{cap})$; and (d) the height of maximum K_m is above 500 m and $K_m(500 \text{ m}) > K_m(\text{cap})$. The dashed red line is the capping value based on wind speed at 500 m, and in (c) and (d), the adjusted K_m profiles are the blue dashed curves.

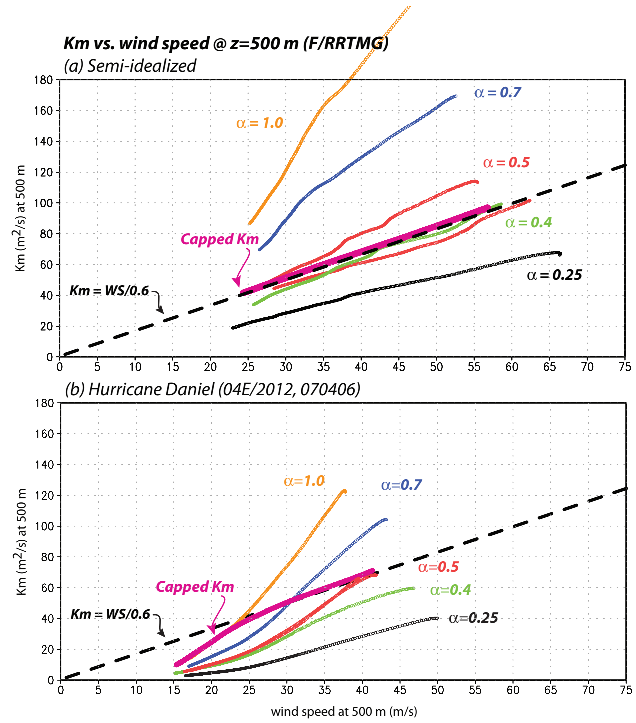

FIG. 12. Eddy diffusivity (m^2 s^{-1}) vs. wind speed (m s^{-1}) at 500 m for simulations using Ferrier/RRTMG with Capped K_m (purple) and various values of α for (a) semi-idealized runs with 302.5 K SST; (b) real-data runs of Hurricane Daniel (2012 04E), initialized on 04 July at 0600 UTC.

eddy mixing for all wind speeds.

As could be anticipated, the 10-m wind profile of capped K_m case resembles α=0.4 for this particular case (Fig. 13). The storm intensity and the radius of the 34-kt wind speed produced by these two storms are almost identical. α=1 and α=0.7 produce much broader wind fields while α=0.25 produces the narrowest wind field, consistent with what suggested by their different K_m profiles. Figure 14 depicts the inflow layer structures of these TCs, plotted with respect to radius normalized by the RMW. Consistent with the results of Gopalakrishnan et al. (2013), restricting K_m effectively decreases the boundary layer depth at inner core region, and the capped K_m inflow structure appears acceptable relative to the Zhang et al. (2011b) category 1-5 composite.

The effect of capped K_m is case-dependent, which can represent an advantage of this strategy over the original α approach in that it will not limit mixing in situations in which it might not be excessive. Figure 12b presents results from 2012 hurricane Daniel, a relatively weak East Pacific case, also made using Ferrier and RRTMG. Relative to the semi-idealized experiment, smaller K_m values were generated at each value of WS and α. The capped K_m effectively limited mixing in most of the storm inner core, as evidenced by mixing not exceeding the WS/0.6 line, but not as severely as single values of $\alpha < 0.7$ would have. The capping implies that α was allowed to increase towards one as radius increased from the RMW, which is a logical result.

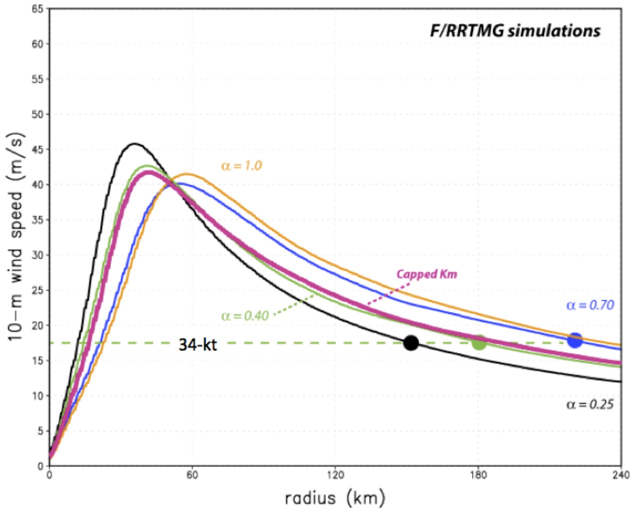

FIG. 13. 10-m tangential wind (m s^{-1}) for simulations with Ferrier MP scheme and α=1.0 (yellow), α=0.7 (blue), α=0.4 (green), α=0.25 (black), and capped K_m (purple).

This modified GFS PBL has been provided to the HWRF developers and tested against retrospective cases. As part of a suite of physics improvements (including the adoption of RRTMG radiation), the modification has been found to improve forecast skill. As a consequence, the modification has been incorporated into the 2015 version of the operational HWRF model.

4. Summary and conclusion

Bu et al. (2014) demonstrated that cloud-radiative forcing (CRF) can exert a substantial influence on numerically simulated TCs, especially with respect to the storm's horizontal scale. We further demonstrated that the radiation scheme employed by the operational HWRF model, which derived from the old GFDL parameterization, was very deficient in handling CRF, to the point that it was essentially absent. However, when the HWRF model was applied to historical cases using a more realistic radiation package, model skill with respect to important storm characteristics such as intensity, position and size was found to be degraded. Our investigation of this phenomenon led us to focus on the planetary boundary layer (PBL) scheme and how it was also influencing storm size, in cooperation and competition with CRF.

Specifically, we found TC structure and intensity to be sensitive to the PBL parameterization, particularly the manipulation of the magnitude and vertical structure of the eddy mixing. Observations suggested that this mixing as produced by the GFS PBL scheme used operationally in the HWRF model to be excessive, with the boundary layer depths it identifies also being too deep, at least within the hurricane inner core. The PBL-generated mixing in this scheme can be tuned via the parameter α, which was added several years ago to (1), the equation that generates the vertical profile of momentum diffusivity. In the current operational model, α is set to 0.7, although Gopalakrishnan et al. (2013) suggested α=0.25 as yielding K_m values and PBL depths that are more consistent with the observations. The larger value of α was selected because it improved the forecast skill of the operational model.

Our analysis suggested that the large value of α used in the operational model was essentially compensating for the lack of cloud-radiative forcing in the HWRF model. As a consequence, when the radiation issue was fixed, the model TCs developed a positive size bias, leading to poorer intensity and position forecasts. At this point, two things become important: to explain how and why PBL mixing influences storm size, and to identify a better, more surgical approach to limiting mixing within the hurricane inner core.

We have come to appreciate that the PBL scheme influences storm size indirectly, in a manner that is actually very similar to the impact of CRF. Eddy mixing of water vapor helps to transport water to the top of the boundary layer. There, the relative humidity is elevated, and convective activity is provoked – presuming environmental conditions (moisture content, vertical stability) – are sufficiently favorable. The convective activity indirectly excited by the vertical moisture transport

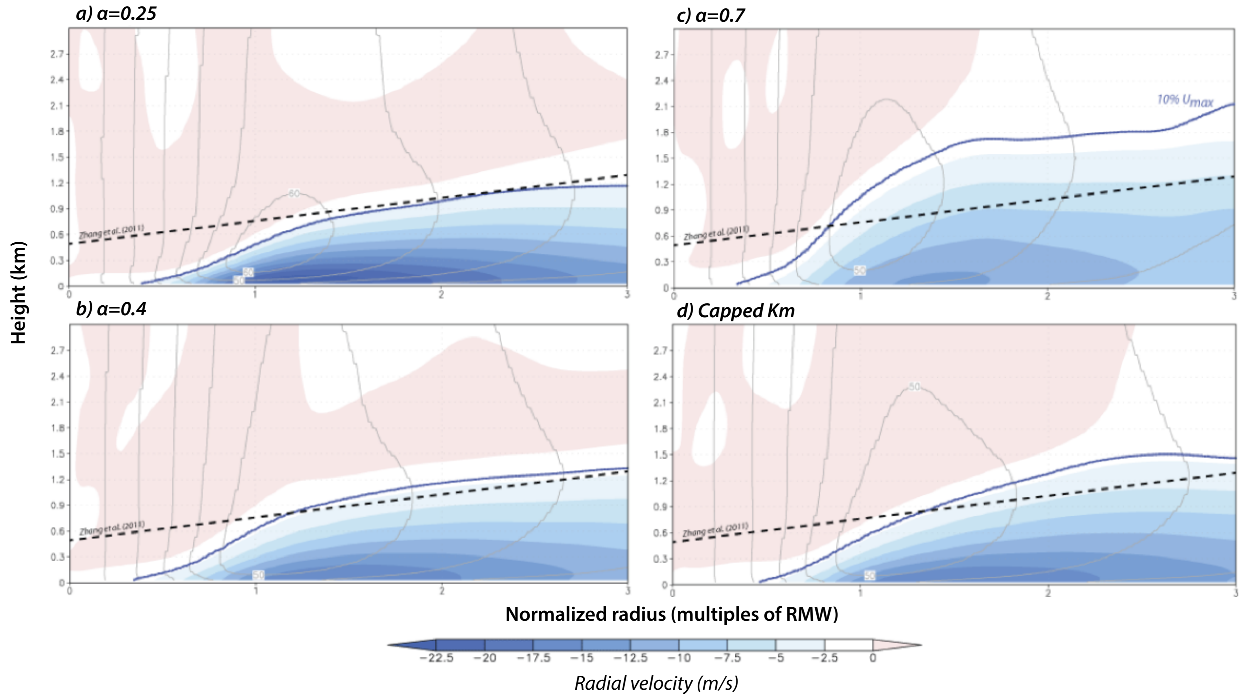

FIG. 14. Radial wind (shaded, m s^{-1}) and tangential wind (contoured, m s^{-1}) versus radius (expressed as multiples of the RMW) for simulations using Ferrier/RRTMG with α equal to (a) 0.25; (b) 0.4; and (c) 0.7; and (d) capped K_m. Solid blue line indicates the PBL depth, based on the 10% of the maximum inflow speed criterion. Black dashed line crudely depicts inflow depth from a Zhang et al. (2011b) category 1-5 composite (their Fig. 10).

generates the heating that broadens the wind field. Thus, a compelling parallel is seen with respect to CRF, the difference being that the heating associated with in-cloud warming was focused above the boundary layer while the PBL influence is essentially bottom-up.

Examination of retrospective cases made using the HWRF model suggested to us that TCs are not always sensitive to α. We have come to understand that the sensitivity is diminished when the TC environment is generally less favorable. We demonstrated that via experiments in which the sea-surface temperature (SST) was reduced. Lower SSTs mean smaller moisture availabilities, and less vertical moisture diffusion, other factors being equal. Our analyses indicate that the vertical moisture flux is the controlling factor.

Within the GFS PBL scheme, the current implementation of the α factor to control excessive hurricane core mixing is attractively simple but has some serious deficiencies, as noted above. We developed new computational method to prevent K_m from being too large when the wind speed is high in a manner that also prevents the scheme from artificially suppressing mixing beyond the hurricane inner core. This scheme was adopted for inclusion in the 2015 release of HWRF and has been selected for the operational configuration.

Acknowledgments. The authors gratefully acknowledge the assistance of Drs. Ligia Bernardet, Mrinal Biswas, Gregory Thompson, Christina Holt, and Vijay Tallapragada, and the support of the Developmental Testbed Center. This work was supported by the National Atmospheric and Oceanic Administrations Hurricane Forecast Improvement Program (HFIP) under Grant NA12NWS4680009 and by the National Aeronautics and Space Administrations Hurricane Science Research Program under Grant NNX12AJ83G.

REFERENCES

Braun, S. A. and W.-K. Tao, 2000: Sensitivity of high-resolution simulations of Hurricane Bob (1991) to planetary boundary layer parameterizations. *Mon. Wea. Rev.*, **128**, 3941–3961.

Bu, Y. P., R. G. Fovell, and K. L. Corbosiero, 2014: Influence of cloud-radiative forcing on tropical cyclone structure. *J. Atmos. Sci.*, **71**, 1644–1662, doi:10.1175/JAS-D-13-0265.1.

Cao, Y., R. G. Fovell, and K. L. Corbosiero, 2011: Tropical cyclone track and structure sensitivity to initialization in idealized simulations: A preliminary study. *Terrestrial, Atmopsheric and Oceanic Sciences*, **22 (6)**, 559–578.

Emanuel, K. A., 1986: An air-sea interaction theory for tropical cyclones. Part I: Steady-state maintenance. *J. Atmos. Sci.*, **43 (6)**, 585–605.

Ferrier, B. S., Y. Jin, T. Black, E. Rogers, and G. DiMego, 2002: Implementation of a new grid-scale cloud and precipitation scheme in NCEP Eta model. *15th Conf. On Numerical Weather Prediction*, San Antonio, TX, Amer. Meteor. Soc., 280–283.

Fovell, R. G. and co authors, 2015: Influence of cloud microphysics and radiation on tropical cyclone structure and motion. *Multiscale Convection-Coupled Systems in the Tropics*, Amer. Meteor. Soc., Meteor. Monogr., in press.

Fovell, R. G., K. L. Corbosiero., A. Seifert, and K. N. Liou, 2010: Impact of cloud-radiative processes on hurricane track. *Geophys. Res. Lett.*, **37 (7)**.

Gopalakrishnan, S. G., S. Goldenberg, T. Quirino, X. Zhang, R. Marks, K. S. Yeh, R. Atlas, and V. Tallapragada, 2012: Toward improving high-resolution numerical hurricane forecasting: influence of model horizontal grid resolution, initialization, and physics. *Wea. Forecasting*, **27 (3)**, 647–666.

Gopalakrishnan, S. G., F. Marks, J. A. Zhang, X. Zhang, J.-W. Bao, and V. Tallapragada, 2013: A study of the impacts of vertical diffusion on the structure and intensity of the tropical cyclones ssing the high resolution HWRF system. *J. Atmos. Sci.*, 120813120734006.

Hill, K. A. and G. M. Lackmann, 2009: Analysis of idealized tropical cyclone simulations using the Weather Research and Forecasting model: Sensitivity to turbulence parameterization and grid spacing. *Mon. Wea. Rev.*, **137 (2)**, 745–765.

Hong, S.-Y. and H.-L. Pan, 1996: Nonlocal boundary layer vertical diffusion in a medium-range forecast model. *Mon. Wea. Rev.*, **124 (10)**, 2322–2339.

Iacono, M. J., J. S. Delamere, E. J. Mlawer, M. W. Shephard, S. A. Clough, and W. D. Collins, 2008: Radiative forcing by long-lived greenhouse gases: Calculations with the AER radiative transfer models. *J. Geophys. Res.*, **113 (D13)**, D13 103.

Klemp, J. B. and R. B. Wilhelmson, 1978: The simulation of three-dimensional convective storm dynamics. *J. Atmos. Sci.*, **35 (6)**, 1070–1096.

Nolan, D. S., D. P. Stern, and J. A. Zhang, 2009a: Evaluation of Planetary Boundary Layer Parameterizations in Tropical Cyclones by Comparison of In Situ Observations and High-Resolution Simulations of Hurricane Isabel (2003). Part II: Inner-Core Boundary Layer and

Eyewall Structure. *Mon. Wea. Rev.*, **137 (11)**, 3675–3698.

Nolan, D. S., J. A. Zhang, and D. P. Stern, 2009b: Evaluation of Planetary Boundary Layer Parameterizations in Tropical Cyclones by Comparison of In Situ Observations and High-Resolution Simulations of Hurricane Isabel (2003). Part I: Initialization, Maximum Winds, and the Outer-Core Boundary Layer. *Mon. Wea. Rev.*, **137 (11)**, 3651–3674.

Ooyama, K., 1969: Numerical simulation of the life cycle of tropical cyclones. *J. Atmos. Sci.*, **26**, 3–40, URL `http://dx.doi.org/10.1175\%2F1520-0469\%281969\%29026\%3C0003\%3ANSOTLC\%3E2.0.CO\%3B2`.

Smith, R. K., 1968: The surface boundary layer of a hurricane. *Tellus*, 473–484, URL `http://onlinelibrary.wiley.com/doi/10.1111/j.2153-3490.1968.tb00388.x/abstract`.

Smith, R. K. and G. L. Thomsen, 2010: Dependence of tropical-cyclone intensification on the boundary-layer representation in a numerical model. *Quart. J. Roy. Meteor. Soc.*, **136 (652)**, 1671–1685.

Thompson, G., P. R. Field, R. M. Rasmussen, and W. D. Hall, 2008: Explicit forecasts of winter precipitation using an improved bulk microphysics scheme. Part II: Implementation of a new snow parameterization. *Mon. Wea. Rev.*, **136 (12)**, 5095–5115.

Troen, I. and L. Mahrt, 1986: A simple model of the atmospheric boundary layer; sensitivity to surface evaporation. *Bound-Lay. Meteorol.*, **37 (l)**, 129–148.

Van Sang, N., R. K. Smith, and M. T. Montgomery, 2008: Tropical-cyclone intensification and predictability in three dimensions. *Quart. J. Roy. Meteor. Soc.*, **134 (632)**, 563–582, URL `http://dx.doi.org/10.1002/qj.235`.

Zhang, J. A., F. D. Marks, M. T. Montgomery, and S. Lorsolo, 2011a: An estimation of turbulent characteristics in the low-level region of intense hurricanes Allen (1980) and Hugo (1989). *Mon. Wea. Rev.*, **139 (5)**, 1447–1462.

Zhang, J. A., R. F. Rogers, D. S. Nolan, and F. D. Marks, 2011b: On the characteristic height scales of the hurricane boundary layer. *Mon. Wea. Rev.*, **139 (8)**, 2523–2535.